Weather and Climate Extremes 35 (2022) 100415

Contents lists available at ScienceDirect

Weather and Climate Extremes

journal homepage: www.elsevier.com/locate/wace

Assessing the potential for crop albedo enhancement in reducing heatwave frequency, duration, and intensity under future climate change

Jatin Kala [a,b,*], Annette L. Hirsch [b], Tilo Ziehn [c], Sarah E. Perkins-Kirkpatrick [e,b], Martin G. De Kauwe [d,b], Andy Pitman [b]

[a] Environmental and Conservation Sciences, Centre for Climate-Impacted Terrestrial Ecosystems, Harry Butler Institute, Murdoch University, Murdoch, WA 6150, Australia
[b] Australian Research Council Centre of Excellence for Climate Extremes, University of New South Wales, NSW 2052, Australia
[c] Commonwealth Scientific and Industrial Research Organisation, Aspendale, VIC 3195, Australia
[d] School of Biological Sciences, University of Bristol, Bristol, BS8 1TQ, UK
[e] School of Science, University of New South Wales Canberra, ACT, Australia

ARTICLE INFO

Keywords:
Land surface radiation management
Heatwaves
Crop albedo

ABSTRACT

Adapting to the impacts of future warming, and in particular the impacts of heatwaves, is an increasingly important challenge. One proposed strategy is land-surface radiation management via crop albedo enhancement. This has been argued to be an effective method of reducing daily hot temperature extremes regionally. However, the influence of crop albedo enhancement on heatwave events, which last three or more days, is yet to be explored and this remains an important knowledge gap. Using a fully coupled earth system model with 10 ensemble members, we show that crop albedo enhancement by up to +0.1 reduces the frequency of heatwave days over Europe and North America by 10 to 20 days; with a larger reduction over Europe under a future climate driven by SSP2-4.5. The average temperature anomaly during heatwaves (the magnitude of the event), is reduced by 0.8 °C to 1.2 °C where the albedo was enhanced, but reductions in mean heatwave duration are limited. There was a marked reduction in the mean annual cumulative heatwave intensity across most of Eurasia and North America, ranging from 32 °C to as high as 80 °C in parts of southern Europe. These changes were largely driven by a reduction in net radiation, decreasing the sensible heat flux, which reduces the maximum temperature, and therefore, heatwave frequency and intensity. These changes were largely localised to where the albedo enhancement was applied with no significant changes in atmospheric circulation or precipitation, which presents advantages for implementation. While our albedo perturbation of up to +0.1 is large and represents the likely upper limit of what is possible with more reflective crops, and we assume that more reflective crops are grown everywhere and instantly, these results provide useful guidance to policy makers and farmers on the maximum possible benefits of using more reflective crops in limiting the impacts of heatwaves under future climate.

1. Introduction

Several regions around the world are expected to experience higher levels of warming relative to global warming targets, especially over land (Seneviratne et al., 2016, 2021). Under current rates of warming, global warming of 1.5 °C relative to pre-industrial levels is expected to be reached and exceeded by 2032–2050 and many regions over land have already experienced regional warming levels of 1.5 °C or higher (Allen et al., 2018; Seneviratne et al., 2021). Therefore mitigation and adaptation of both current and future warming remains necessary. Of particular importance are heatwave events, which are increasing in frequency, intensity and duration, with the increase in frequency being the most significant in almost all regions of the globe (Perkins-Kirkpatrick and Lewis, 2020). The impacts of these heatwave events can be very significant, including impacts on human health (e.g., McMichael and Lindgren, 2011), public infrastructure (e.g., Rübbelke and Vögele, 2011; McEvoy et al., 2012), wildfires (e.g., Westerling et al., 2006; Jyoteeshkumar reddy et al., 2021), agriculture (e.g., van

* Corresponding author at: Environmental and Conservation Sciences, Centre for Climate-Impacted Terrestrial Ecosystems, Harry Butler Institute, Murdoch University, Murdoch, WA 6150, Australia.
E-mail address: J.Kala@murdoch.edu.au (J. Kala).

https://doi.org/10.1016/j.wace.2022.100415
Received 29 September 2021; Received in revised form 19 January 2022; Accepted 26 January 2022
Available online 9 February 2022

der Velde et al., 2010; Asseng et al., 2015; Herold et al., 2018), ecosystem services (e.g., Ruthrof et al., 2018), human health (e.g., Chambers, 2020), infrastructure and energy supply (e.g., Klimenko et al., 2020), and many other sectors.

Several strategies have been proposed to mitigate the risk of heatwaves, including the deliberate geoengineering of the earth's climate system to reduce warming. Geoengineering can be classified into two broad categories: carbon dioxide removal from the atmosphere, and changes in the earth's energy balance (Keith, 2000). Methods to alter the earth's energy balance are generally based on reductions in incoming shortwave radiation, e.g., sulphate aerosols injection in the stratosphere, desert albedo modification, marine cloud brightening. These large-scale solar radiation management (SRM) methods aim to reduce warming globally (Keith, 2000; Kravitz et al., 2021) although they have also been criticised (e.g., Lawrence et al., 2018).

On the other hand, land-surface radiation management, which involves the use of alternative and more reflective crop varieties and/or no-till farming and irrigation methods, aims to induce regional cooling rather than a reduction in global warming (Davin et al., 2014; Wilhelm et al., 2015; Thiery et al., 2017; Hirsch et al., 2017; Seneviratne et al., 2018; Hirsch et al., 2018; Thiery et al., 2020; Kala and Hirsch, 2020). There are several advantages of land based SRM techniques relative to large-scale SRM. For example, large areas of land are already under direct human management for cropping and if those crops could be brightened, this might lead to local cooling at little cost, without endangering crop yield, or even potentially increasing yields (Genesio et al., 2021). Further, if specific regions are vulnerable to heat extremes these can be directly targeted by land-based SRM. A further advantage is that the implementation of land-based SRM is a matter of national rather than international policy given the impacts are largely local. Finally, in contrast to large-scale SRM techniques, the science of land SRM is relatively well known and can be considered low risk.

The use of more reflective (higher albedo) crops to induce regional cooling is supported by observations. For example, Genesio et al. (2021) investigated the energy balance of lower chlorophyll soybean crops (lighter colour and higher albedo) as compared to a higher chlorophyll soybean variety (darker colour and lower albedo), and showed that differences in mean daily temperature and sensible heat flux measured over the two different crops were as high as −6 °C and −80 W m^{-2}, respectively. When averaged over the growing season crop cycle (May-September), Genesio et al. (2021) estimate that the reduction in shortwave radiative forcing by using soybean crops with higher albedo is 4.1 ± 0.6 W m^{-2}. They therefore argue that enhanced crop albedo should be considered as an effective policy option in mitigating against regional warming, while maintaining, or even potentially increasing crop yield.

Recent work using earth system models to investigate the effectiveness of land based SRM techniques have shown that crop albedo enhancement could be very effective in mitigating against regional warming (Hirsch et al., 2017, 2018; Kala and Hirsch, 2020). However, the focus of this work has mostly been on changes in the hottest day of the year and/or changes in maximum temperature averaged over summer. Some of the most significant impacts are not just related to the warmest day of the year, but rather to heatwave events, which are generally defined as a minimum of three consecutive days during which a locally-based extreme temperature threshold is exceeded (Perkins and Alexander, 2013). Reductions in the intensity, duration and frequency of heatwaves in regions associated with crops could have substantial benefits. We also note that most of the work examining the effectiveness of crop albedo enhancement globally have been carried predominantly using only one earth system model, the Community Earth System model (CESM) (Hirsch et al., 2017, 2018). Consequently there is value in examining the robustness of crop albedo enhancement using different earth system models, with specific focus on heatwaves.

In this paper we investigate the effectiveness of crop albedo enhancement in reducing the intensity, duration, and frequency of heatwaves using an ensemble of simulations from the Australian Community Climate and Earth Systems Simulator (ACCESS) Earth System Model version 1.5 (ACCESS-ESM1.5), an earth system model contributing to the Coupled Model Intercomparison Project Phase 6 (CMIP6). We first assess model skill in simulating different heatwave metrics for historical climate against gridded observational estimates. Simulations are carried out with enhanced crop albedo under future climate driven by SSP2-4.5 and we analyse changes in the heatwave metrics and their drivers.

2. Methods

2.1. Model description

ACCESS-ESM1.5 (Ziehn et al., 2020) is comprised of several component models. The atmospheric model is the UK Met Office Unified Model at version 7.3 (Martin et al., 2010, 2011) with the original land surface model, the joint UK Land Environment Simulator, replaced with the Community Atmosphere Biosphere Land Exchange (CABLE) model version 2.4 (Kowalczyk et al., 2013). The model uses a horizontal resolution of 1.875° × 1.25° at the surface and 38 vertical levels in the atmosphere. The ocean component is the NOAA/GFDL Modular Ocean Model at version 5 (Griffies, 2014) with the same configuration as the ocean model component of ACCESS1.0 and ACCESS1.3 (Bi et al., 2013) using a 1° resolution (but finer between 10S-10N and in the Southern Ocean) and 50 vertical levels. Sea ice is simulated using the LANL CICE4.1 model (Hunke and Lipscomb, 2010). Coupling of the ocean and sea-ice to the atmosphere is through the OASIS-MCT coupler (Valcke, 2013) with a coupling frequency of three hours. The physical climate model configuration used here is very similar to the version (ACCESS1.3) that contributed to the Coupled Model Intercomparison Project Phase 5 (CMIP5) (Bi et al., 2013). The carbon cycle is included in ACCESS through the CABLE land surface model and its biogeochemistry module, CASA-CNP (Wang et al., 2010), and through the World Ocean Model of Biogeochemistry and Trophic-dynamics (Oke et al., 2013).

The Australian community model CABLE simulates the fluxes of momentum, heat, water and carbon at the surface. The biogeochemistry module CASA-CNP simulates the flow of carbon and the nutrients nitrogen and phosphorus between three plant biomass pools (leaf, wood, root), three litter pools (metabolic, structural, coarse woody debris), three organic soil pools (microbial, slow, passive), one inorganic soil mineral nitrogen pool and three phosphorus soil pools (Wang et al., 2010). In the CABLE configuration applied here, we use 10 vegetated types (i.e., plant functional types) and three non-vegetated types. CABLE calculates gross primary production (GPP) and leaf respiration at every time step using a two-leaf canopy scheme (Wang and Leuning, 1998) as a function of the leaf area index (LAI). Our set-up uses a simulated (prognostic) LAI based on the size of the leaf carbon pool and the specific leaf area. Daily mean GPP and leaf respiration values are then passed onto CASA-CNP to calculate daily respiration fluxes and the flow of carbon and nutrients between the pools. Similar to the previous version, ACCESS-ESM1 (Ziehn et al., 2017; Law et al., 2017), we ran simulations with both nitrogen and phosphorus limitation enabled.

The ACCESS-ESM1.5 model has been evaluated against ERA-Interim re-analysis (Dee et al., 2011), and results show a Southern ocean warm bias during both summer and winter, which is a longstanding issue with the model. Substantial biases include a warm bias over India during the northern hemisphere winter, as well as across the equatorial land masses and North America, and cold biases over North Africa and the Arabian Peninsula . The largest precipitation biases in ACCESS-ESM1.5 occur over the inter-tropical convergence zone, with a tendency for wet biases over the Maritime continent, and dry bias over India during the monsoon season (Ziehn et al., 2020).

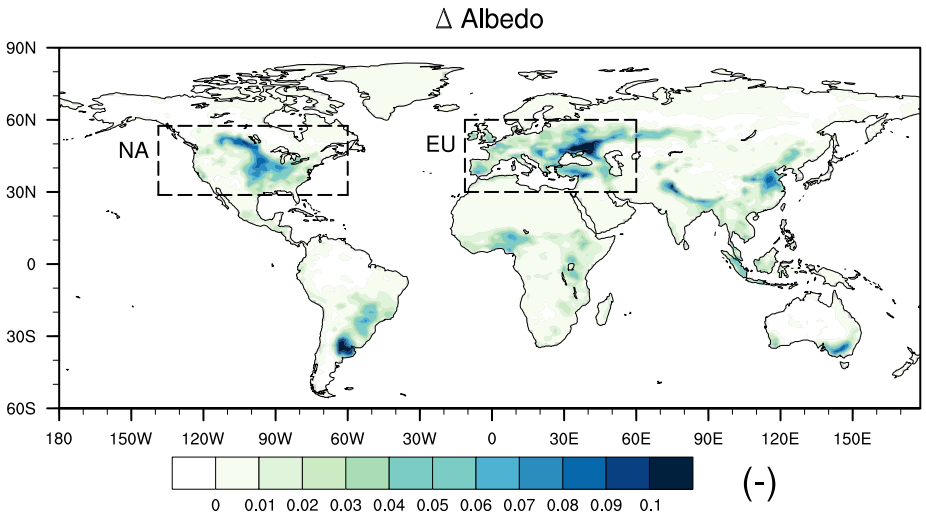

Fig. 1. Change in surface albedo (experiment minus control), averaged across all 10 ensemble members over summer during May to September (MJJAS) (northern hemisphere) and November to March (NDJFM) (southern hemisphere) over the period 2021–2099. The EU and NA boxes denote Europe and North America respectively, where further time series analysis is carried out.

2.2. Experiments with enhanced crop albedo

Five Shared Socio-economic Pathways (SSP) have been developed for CMIP6, ranging from best case SSP1 (Sustainability: taking the green road), to worst case SSP5 (fossil-fuelled development: taking the highway), with three intermediate SSPs, and each of five SSPs also have a number of enhanced radiative forcings by 2100, ranging from 1.9 to 8.5 W m^{-2} (Meinshausen et al., 2020). Due to computational limitations, we were only able to run simulations for one future scenario, and we deliberately choose a scenario which is in the middle, in terms of both the SSP and the radiative forcing. This was SSP2-4.5 (O'Neill et al., 2016), which is a "middle-of-the-road" scenario, combining intermediate societal vulnerability with an intermediate forcing level of 4.5 W m^{-2}. We used 10 ensemble members continuing from 10 historical simulations (years 1850–2014). The historical simulations were initialised at different times from the pre-industrial-control run (20 years apart). This method of ensemble generation provides sufficient model spread (shown later in the manuscript in the evaluation section).

We first ran the control simulations which did not involve crop albedo enhancement. For the experiments, crop albedo enhancement was applied from the year 2021 onwards to 2100, assuming no prior implementation, following the same methodology as Hirsch et al. (2017). In the CABLE land surface model within ACCESS-ESM1.5, the albedo of different plant functional types (PFTs) is based on the absorption of visible and near infrared radiation for sunlit and shaded leaves separately and key input parameters for the vegetation albedo scheme include the leaf transmittance and reflectance values (Kala et al., 2014; Wang et al., 2011). We carry out experiments with enhanced crop albedo by doubling the reflectance and halving the transmittance of all C3 crops (i.e, crops which use C3 photosynthesis during which the first carbon compound produced contains three carbon atoms). We note that C4 crops (i.e., crops which use C4 photosynthesis during which the first carbon compound produced contains four carbon atoms) are not implemented in ACCESS-ESM1.5. The crop albedo enhancement is not static in time, but follows the seasonal cycle and is highest when crops are most active during summer and the leaf area index is maximum. This is illustrated in Fig. 1 showing a maximum increase in crop albedo of approximately 0.1 in summer averaged between 2021–2099 (Fig. 1). This is the same maximum albedo perturbation as applied by Hirsch et al. (2017) who carried out global simulations using CESM, and Kala and Hirsch (2020) who carried out regional simulations using a regional model.

A perturbation of up to +0.1 represents the upper limit of what is currently possible with variations in major crops. This includes observed variations in albedo of 0.01 to 0.06 across barley cultivars (Breuer et al., 2003; Febrero et al., 1998), 0.02 across soybean cultivars (Breuer et al., 2003), 0.05 across sorghum cultivars (Grant et al., 2003), 0.06 to 0.1 in wheat cultivars (Uddin and Marshall, 1988), 0.08 to 0.1 across maize, sunflower and oat cultivars (Breuer et al., 2003; Hatfield and Carlson, 1979) and 0.14 for rye cultivars (Breuer et al., 2003). We note that the ACCESS-ESM1.5 simulations also include annual changes in land-cover based on the LUH2 data-set (Hurtt et al., 2020). We examined changes in albedo at the start of the experiments (2021) as compared to the end (2099), and changes were minor (not shown), with a slight increase towards 2099 due to crop expansion.

For statistical significance testing of differences between the experiments and the control, we use the student t-test at 95% confidence interval, with Walker's test for field significance (Wilks, 2006), a commonly used statistical approach for field significance in land–atmosphere studies (e.g., Lorenz et al., 2016).

2.3. Heatwave metrics

The definition of a heatwave depends on the sector, however, two definitions are most widely adopted within the earth sciences, both based on percentiles. The first definition is based on maximum temperature alone, and a heatwave event is defined as three or more consecutive days when the daily maximum temperature exceeds the 90th percentile of maximum temperature at a particular location, with the percentiles computed for each day of the year with a 15-day window, over a reference period of at least 30 years, as described in Perkins and Alexander (2013). This definition of heatwaves has been used in previous work focusing on heatwaves using the ACCESS model (Kala et al., 2016) as well as recent observational studies (Perkins-Kirkpatrick and Lewis, 2020). The second definition is based on the Excess Heat Factor (EHF), which is computed using both maximum and minimum temperature and takes into consideration acclimatisation and was principally formulated for human health outcomes of heatwaves (Nairn and Fawcett, 2015). Similarly, using the EHF, a heatwave event is defined as 3 or more consecutive days with positive EHF (Perkins and Alexander, 2013).

Since this study does not explicitly focus on health implications of heatwaves, we chose the first definition based on maximum temperature alone rather than the EHF, as our focus is on the broad implications of heatwaves. Additionally, for this study, we only focus

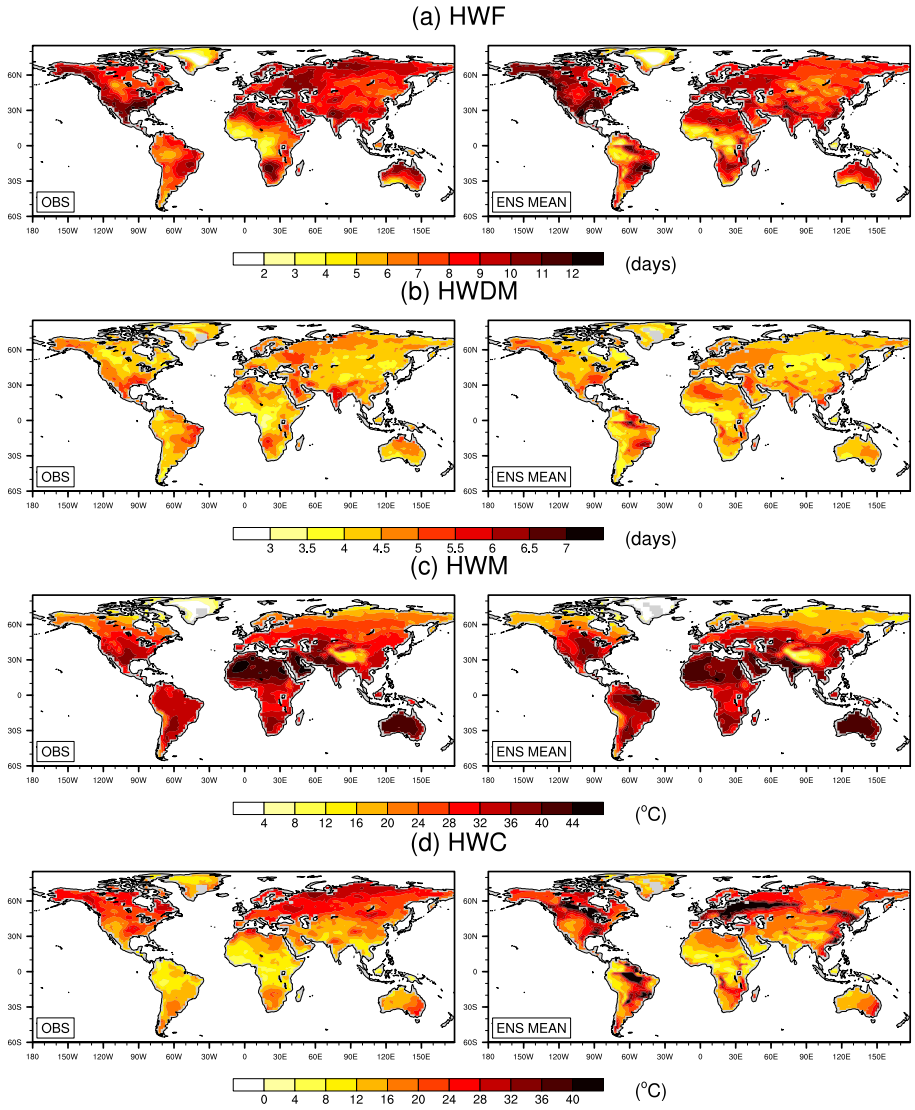

Fig. 2. Observed heatwave metrics from the Berkeley dataset (OBS; left column) and ACCESS-ESM1.5 ensemble mean (ENS MEAN; right column), averaged over the period 1950–2014 during summer (MJJAS northern hemisphere and NDJFM southern hemisphere). (a) HWF is number of heatwave days; (b) HWDM is mean heatwave duration; (c) HWM is the heatwave magnitude, i.e., average temperature of heatwave events; (d) HWC is the cumulative heat, i.e., the sum of the anomalies between the heatwave temperature and the 90th percentile of maximum temperature.

on heatwaves which occur during an extended summer period covering 5 months (November to March for the southern hemisphere and May to September for the northern hemisphere) and do not analyse heatwaves during other seasons as we are focusing on the maximum potential benefits of crop albedo enhancement during the hottest part of the year when impacts of heatwaves are most significant.

We consider 4 heatwave properties: the heatwave frequency (HWF), which is the total number of heatwave days per year during summer, the mean heatwave duration (HWDM; we note here that the most prior studies refer to maximum heatwave duration, termed HWD, hence we use HWDM here to avoid confusion) defined as the mean duration of heatwaves, the heatwave magnitude (HWM) defined as the average temperature of all heatwaves events, and the heatwave cumulative heat (HWC), which is the sum of the temperature anomalies (the difference between the maximum temperature during a heatwave day and the 90th percentile of maximum temperature on that day) of all events during a season. More details about HWC can be found in Perkins-Kirkpatrick and Lewis (2020).

2.4. Observational temperature data-set

To evaluate the skill of ACCESS-ESM1.5 in simulating heatwaves during the historical period, we use the Berkeley Earth gridded temperature data-set (Rohde et al., 2013), a gridded observational data-set of daily maximum and minimum temperature which has been used in recent observational studies of heatwaves (Perkins-Kirkpatrick and Lewis, 2020). The Berkeley Earth dataset was used in this study as it is a more complete data-set of daily temperature extremes and comparable to the more widely used data-sets (Perkins-Kirkpatrick and Lewis, 2020).

The resolution of the Berkeley data is 1.0° x1.0° resolution which is a finer resolution than ACCESS-ESM1.5 which has a resolution of 1.875° × 1.25°, and hence, the Berkeley data-set was interpolated to the coarser resolution. For model evaluation, we computed the yearly summer heatwave metrics over the period 1950–2014, using a base period of 65 years also between 1950–2014 to compute the 90th percentiles of maximum temperature (TMAX) for every calendar day of the year. While previous studies typically use a 30 year reference

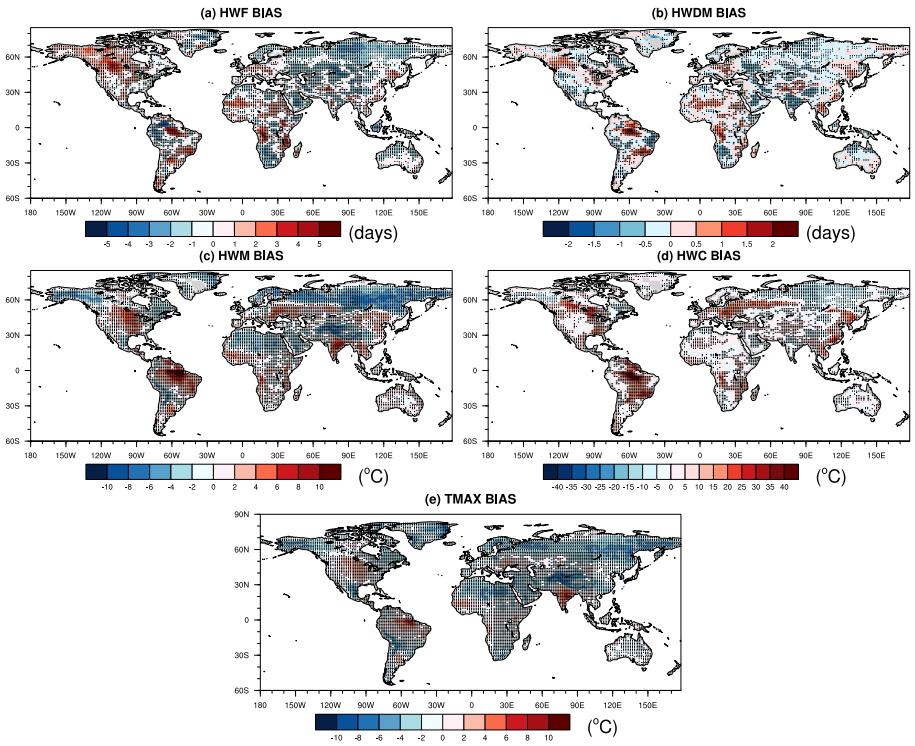

Fig. 3. Bias in (a) HWF; (b) HWDM; (c) HWM; (d) HWC, (e) maximum temperature (TMAX) between ACCESS-ESM1.5 and the Berkeley dataset (model minus observations), averaged over the period 1950–2014 during summer (MJJAS northern hemisphere and NDJFM southern hemisphere). Stippling denotes grid cells where 9 or more of the 10 ensembles have the same sign in the bias.

period to compute the percentiles (e.g., Kala et al., 2016), a 65 year period was chosen to better account for decadal variability. We note that the Berkeley data has missing data, especially in the early part of the record (Perkins-Kirkpatrick and Lewis, 2020) and ACCESS-ESM1.5 data were masked to ensure consistency.

3. Results

3.1. Evaluation of ACCESS-esmv1.5 skill in simulating heatwave metrics

Fig. 2 shows the observed heatwave metrics (OBS; left column), the ensemble mean simulated heatwave metrics (ENS MEAN; right column) averaged over the period 1950–2014 during summer (MJJAS northern hemisphere and NDJFM southern hemisphere), and the bias (model minus observations) is shown in Fig. 3. The spatial pattern of all heatwave metrics is generally well simulated by ACCESS-ESM1.5 (Fig. 2), with the model capturing regions which experience the most frequent, intense and longest heatwave events. There is notable positive bias in the number of heatwave days (HWF) in northern North America of 3 to 4 days (Fig. 3(a)), and similar large biases can be found in equatorial South America and Western Central Africa. However, it should be noted that heatwave metrics near the equator should be treated with caution due to the splitting of the hemispheres to combine the summer season globally, and also the generally small seasonal variation in the 90th percentile of TMAX close to the equator.

The bias in the mean heatwave duration (HWDM; Fig. 3(b)) ranges between −0.5 to 0.5 days, except for some regions close to the equator. Biases in the heatwave magnitude (HWM; Fig. 3(c)) and cumulative heat (HWC; Fig. 3(d)) are more substantial. HWM is under-estimated by 2 to 6 °C in northern Europe north of 60°N; under-estimated by 4 to 8 °C over the Himalayas; over-estimated by 2 to 6 °C in parts of Western Europe and North America between 30°N and 60°N; and over-estimated by 4 to 8 °C over India and south America near the equator. Since the heatwave indices are based on TMAX, we examined biases in the latter as shown in Fig. 3(f), and not surprisingly, the biases in HWM (Fig. 3(c)) are essentially a reflection of the biases in TMAX (Fig. 3(f)). Biases in HWC (Fig. 3(d)) were most prominent in South America near the equator, parts of North America and central Europe and along the east coast of Eurasia. Overall, for all heatwave metrics and TMAX, the biases had consistent signs across the 10 ensemble members as shown by the stippling, showing these are systematic in ACCESS-ESM1.5.

To further investigate the model skill in simulating trends in the heatwave metrics, we examined the time series of the yearly heatwave metrics over Europe (EU) and North America (NA) (refer to boxes in Fig. 1), as illustrated in Fig. 4. We chose these two regions as these showed the largest response to increasing crop albedo (discussed in the next section) and they are also major cropping regions which are particularly susceptible to the impacts of heatwaves (Fischer and Schär, 2010; Russo et al., 2015). Fig. 4 shows both the model ensemble mean (red line) and spread (light red shading) as well as the observations (solid black line), and illustrates that except for 2 to 3 years, the model ensemble spread captures the observed trends reasonably well for both regions for all 4 heatwave metrics, and importantly, the increasing trend in HWF from the 1990s onwards, especially in Europe, is very well captured by ACCESS-ESM1.5.

The large bias in TMAX (Fig. 3(e)) over India is a known issue of ACCESS-ESM1.5 and is related to a significant under-estimation of precipitation associated with the monsoon leading to an overestimation of maximum temperature (Lorenz et al., 2014; Ziehn et al., 2020). The recent intergovernmental panel on climate change 6th assessment report chapter on extremes (Seneviratne et al., 2021) does not explicitly examine heatwave events, but does include an evaluation of the annual hottest temperature by CMIP6 models, and shows a large cold bias over the Himalayas, and as well an under-estimation in northern Europe north of 60N. Although not directly comparable, these are similar to the biases in HWM and TMAX we present here, showing the biases in ACCESS-ESM1.5 are present in most ESMs in CMIP6.

Hirsch et al. (2021) evaluated the skill of CMIP5 and CMIP6 ESMs, including ACCESS-ESM1.5, in simulating the same heatwave metrics against the Berkeley Earth data-set as used in this study. We note

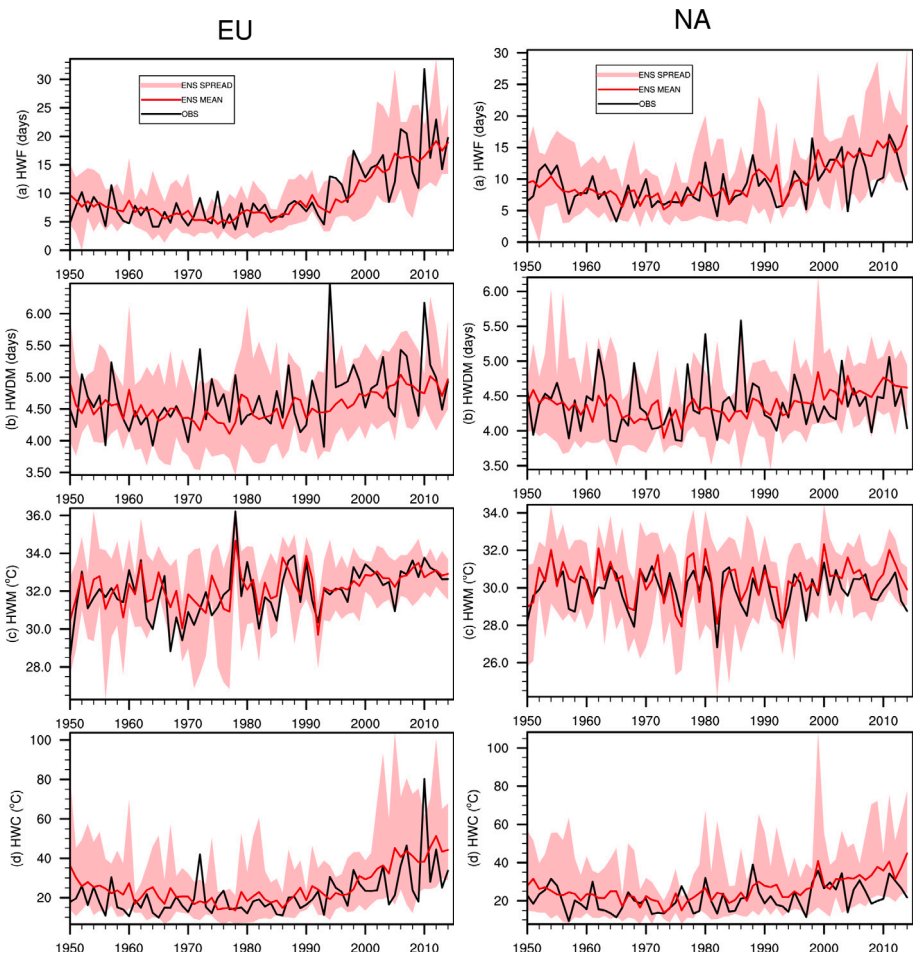

Fig. 4. Yearly time-series (1950–2014) of observed and simulated heatwave metrics for Europe (EU) and North America (NA) (refer boxes in Fig. 1). The solid black line denotes the observations (OBS), the solid red line denotes the ensemble mean (ENS MEAN), and ensemble spread is shown by the light red shading (ENS SPREAD). Panel (a) is HWF; (b) is HWDM; (c) is HWM; and (d) is HWC. (For interpretation of the references to colour in this figure legend, the reader is referred to the web version of this article.)

that they adopted a different definition of heatwaves based on the excess heat factor, which takes into consideration both maximum and minimum temperature, rather than only maximum temperature as used in this study. However, studies have shown that the heatwave events detected and overall trends are likely similar between these two heatwave definitions (Perkins and Alexander, 2013), and hence comparisons are still useful. Hirsch et al. (2021) showed that both CMIP5 and CMIP6 models tend to overestimate HWC, a result we also found with ACCESS-ESM1.5 (Fig. 3(d)). They also report that both CMIP5 and CMIP6 models tend to underestimate HWF across the globe, however, here we show regions of both underestimations and overestimations in ACCESS-ESM1.5 (Fig. 3(a)).

In summary, ACCESS-ESM1.5 shows reasonable skill in simulating heatwave characteristics, with biases well within the range of CMIP5 and CMIP6 models assessed by Hirsch et al. (2021), giving us confidence in the use of the model to examine the influence of crop albedo enhancement on projections of heatwaves under future climate.

3.2. Effect of crop albedo enhancement on heatwave metrics

Fig. 5 shows the changes in the heatwave metrics (experiments with higher crop albedo minus control) during summer averaged over the period 2021–2099 under SSP2-4.5. Increasing crop albedo results in a reduction in HWF, especially over EU and NA by 15 to 20 days and up to 25 days in some regions of southern Europe (Fig. 5(a)). The change in the mean duration (HWDM; Fig. 5(b)), although considered statistically significant over some regions, is generally small and although changes are large over Egypt, these are not statistically significant. There are statistically significant reductions in heatwave magnitude (HWM; Fig. 5(c)) of 0.8 to 1.2 °C over parts of EU and NA. Reductions in the cumulative heat (HWC; Fig. 5(d)) are more widespread across most of Eurasia and North America, ranging from 32 °C to as high as 80 °C in parts of southern Europe. Generally, changes in the southern hemisphere are small and not statistically significant except for parts of southern South America and southeast Australia for HWF and HWC. Overall, the majority of statistically significant changes occurred where the surface albedo was increased, and the highest percentage of statistically significant changes where crop albedo was not increased was for HWC (12%) and lowest for HWDM (7%). This shows that the effects of crop albedo modification are largely local.

We further investigated changes over EU and NA, where reductions in the heatwave metrics were highest and statistically significant (Fig. 5). This is illustrated in Fig. 6 showing the yearly time series of the heatwave metrics averaged over the EU and NA boxes (refer to Fig. 1), with the shading representing the ensemble spread. For HWF, HWDM, and HWC, there is a distinct shift between the control and experiments with enhanced crop albedo in two ways: firstly the ensemble mean for the experiments (solid blue line) is always lower than the ensemble mean for the control (solid red line) throughout the period 2021–2099, and secondly, the upper spread of the control (light red shading above the solid red line), is always separate from the upper spread of the experiment (light blue above the solid blue line). This is however not the case for HWM for both regions, with the ensemble spread between the control and experiment showing much

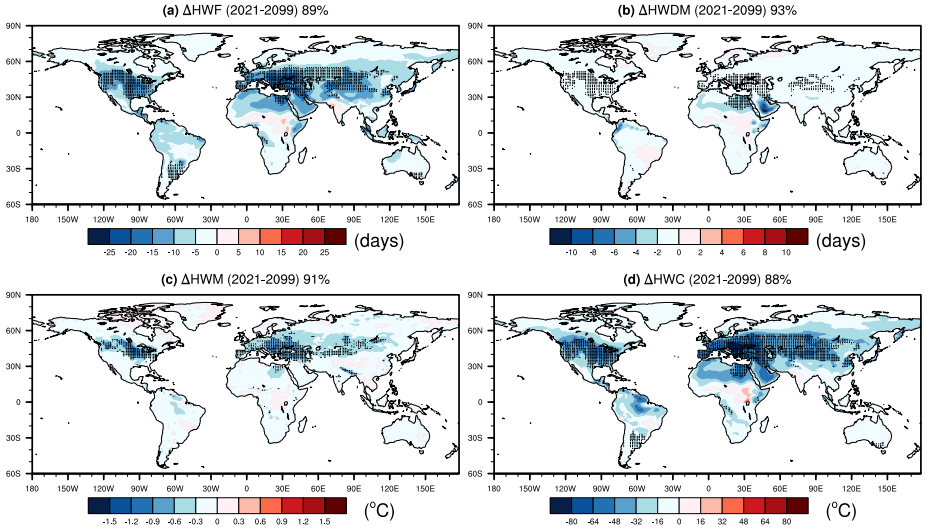

Fig. 5. Change (experiment minus control) in summer (MJJAS northern hemisphere and NDJFM southern hemisphere) heatwave metrics averaged over the period 2021–2099 under SSP2-4.5. Panel (a) is HWF; (b) is HWDM; (c) is HWM; and (d) is HWC. Stippling denotes regions where differences are statistically significant at the 95% level with the Walker's test for field significance. The percentages in the titles denote the percentage of grid cells which show a statistically significant difference where the surface albedo was increased (Fig. 1). For example, 90% means that 90% of grid cells which show a statistically significant difference are grid cells where the surface albedo was increased, and hence, 10% of grid cells show a change where there was no increase in crop albedo.

more overlap, and additionally, for NA, the ensemble mean for the control and experiment tend to merge from 2080 onwards, with the ensemble spread almost completing overlapping by 2099.

3.3. Changes in the surface energy balance

To investigate the mechanisms behind changes in the heatwave metrics, we examined the changes in the surface energy balance, as illustrated in Fig. 7 showing the changes in TMAX, net shortwave radiation, sensible heat flux, latent heat flux, net longwave radiation, and cloud fraction. There is a statistically significant reduction in TMAX where crop albedo is increased (91% of grid cells; Fig. 7(a)). Although there is a slight increase in maximum temperature over India and parts of central Africa, this is not statistically significant. This reduction in maximum temperature, and subsequent changes to the heatwave metrics (Figs. 5 and 6) are driven by a reduction in net shortwave radiation of 15 to 30 W m^{-2} (Fig. 6(b)), which results in a reduction in sensible heat flux of 10 to 25 W m^{-2} (Fig. 6(c)), and changes in latent heat flux were generally small ranging between −5 to 5 W m^{-2} (Fig. 6(d)). There was an increase in net longwave radiation of up to 10 to 15 W m^{-2} (Fig. 6(e)), especially over Europe, and slight increases over India and central Africa. These changes in net longwave radiation were due to changes in cloud fraction (Fig. 7(f)) with higher cloud fraction leading to higher net longwave radiation and vice-versa. The most plausible explanation for this is lower temperature resulting in lower saturation vapour pressure, increasing relative humidity, and therefore condensation and cloud formation. Overall, the effect of higher crop albedo in our simulations on the surface energy balance is straight-forward: higher surface albedo results in lower net shortwave radiation, and although some regions showed an increase in net longwave radiation, this was less than half of the increase in net shortwave radiation, resulting in a reduction in net radiation (net shortwave plus net longwave). This reduced the sensible heat flux, and with only small changes in the latent heat flux, this results in a decrease in maximum temperature and subsequent changes to the heatwave metrics.

3.4. Discussion and conclusions

Heatwaves have very significant impacts on a range of sectors in society. In this study, we investigated using crop albedo enhancement to reduce the impact of heatwave conditions by applying a perturbation of up to +0.1, which represents the upper limit of possible enhancement in crop albedo given existing crop varieties (Hatfield and Carlson, 1979; Uddin and Marshall, 1988; Febrero et al., 1998; Breuer et al., 2003; Grant et al., 2003). We examined the effects on four different properties of heatwaves, the frequency of heatwave days (HWF), magnitude or average temperature of heatwave events (HWM), mean duration (HWDM) and annual cumulative intensity (HWC), using a fully coupled earth system model with 10 ensemble members. We first demonstrated model skill in representing heatwave metrics across the globe when compared against gridded observations; with the model adequately capturing the increasing trend in HWF from the 1990's onwards, especially for Europe where the trend is marked. Results also showed that the sign of the bias for all heatwave metrics, as well as maximum temperature was remarkably consistent between the ensembles, which implies that these biases are systematic, and there is much scope for further model development for ACCESS-ESM1.5.

Our results show a statistically significant reduction in HWF, HWC and HWM, where crop albedo is enhanced, especially over Europe and North America. These results are significant in several aspects. Firstly, the observed increasing trend in HWF over Europe since the 1990's is stark (Fig. 4) as discussed in recent studies (Perkins-Kirkpatrick and Lewis, 2020) and this trend continues in the future (Fig. 6), however, with crop albedo enhancement, HWF is reduced by approximately 10 days on average (Fig. 6(a)) in EU, driven by the reduction in TMAX (Fig. 7(a)) which means fewer days above the climatological 90th percentile and hence lower HWF. Heatwaves in Europe have considerable impacts and these are expected to increase significantly under future climate change especially for southern Europe (Fischer and Schär, 2010; Russo et al., 2015). Crop albedo enhancement could be helpful in reducing the severity of impacts of heatwaves in some regions of Europe. Secondly, our results are largely local, only 7 to 12% of grid cells show a statistically significant change in heatwave properties without crop albedo enhancement at these grid cells. This has obvious advantages with regards to implementation as compared to large scale SRM techniques such as stratospheric aerosol injection which can have significant remote effects, such as changes to the global monsoon circulation (e.g., Sun et al., 2020), large scale changes to the ocean and land carbon cycles (e.g., Tjiputra et al., 2016), changes to

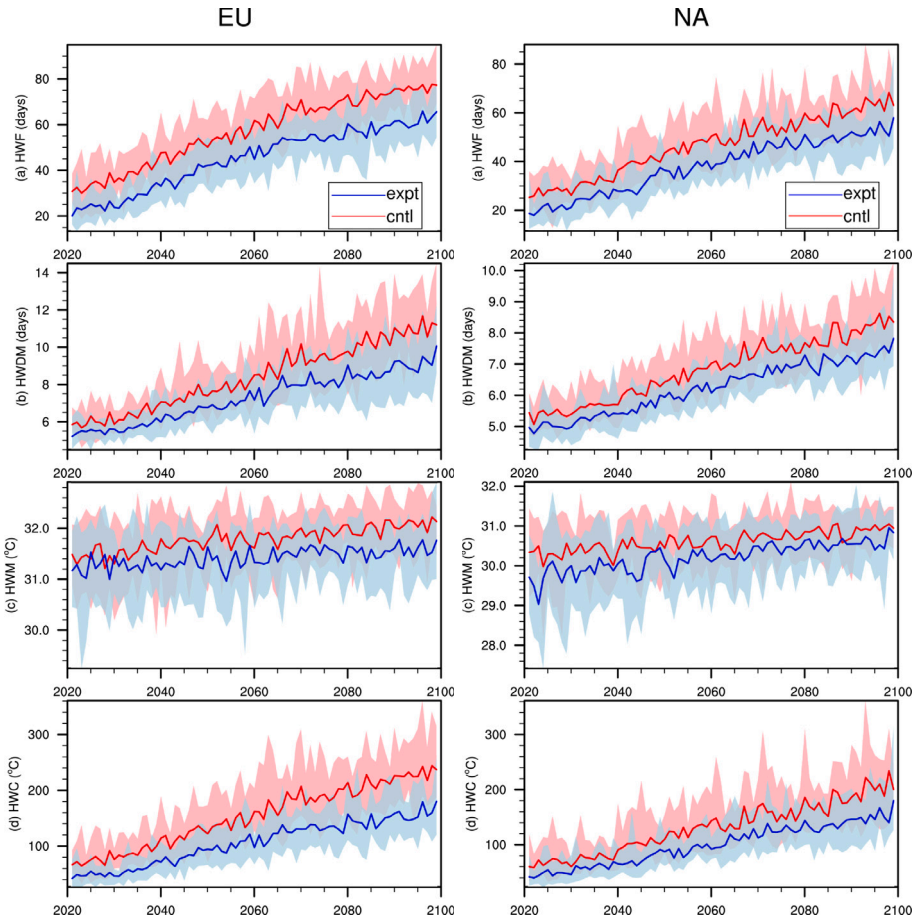

Fig. 6. Yearly time series of heatwave metrics for EU and NA boxes (refer to Fig. 1) from 2021 to 2099 under SSP2-4.5. The light blue shading represents the ensemble spread from the experiment and light red for the control simulations. Panel (a) is HWF; (b) is HWDM; (c) is HWM; and (d) is HWC. (For interpretation of the references to colour in this figure legend, the reader is referred to the web version of this article.)

ocean pH as well as sudden termination effects when implementation is stopped and warming resumes (e.g., Brovkin et al., 2009). We did not find significant changes in precipitation or the atmospheric circulation in our simulations (not shown).

We compared changes in the annual maximum temperature (TXX) from our simulations to those by Hirsch et al. (2017) who used CESM and imposed a similar perturbation of +0.1 in crop albedo, and we found similar maximum reductions of similar orders of magnitude over Europe. Although Hirsch et al. (2017) ran simulations under RCP8.5, whereas we use SSP2-4.5 and we cannot directly compare absolute magnitudes, this consistency between two ESMs which make use of different land surface models is encouraging and provides confidence that the simulations are not model dependent.

Hirsch et al. (2017) reported an overall increase in mean net yearly primary productivity (NPP; grid cell average) of 15 to 30 g C m^{-2} yr^{-1} by increasing crop albedo by 0.1, which represented a percentage increase of 5 to 10%. This was attributed to lower temperatures potentially leading to more optimal conditions for plant growth. We also found an increase in net yearly primary productivity (grid cell average), but of larger magnitude, with an increase of up to 100 to 150 g C m^{-2} yr^{-1}, especially over southern EU and NA, representing a percentage increase of 10 to 20%. We also examined the changes in NPP for C3 crops specifically (rather than grid-cell averages) over summer, and found an increase in NPP of 300, to 400 g C m^{-2} yr^{-1} over southern EU, accompanied by increase in LAI by 0.6 to 1.2. However, we are cautious of these results especially in making inferences about potential yield gains, given the very simple representation of crops in our model, and also the fact that we assumed more reflective crops would have exactly the same physiological parameters as the control other than their reflectance and transmittance, and did not incorporate irrigation or fertilisation application. To adequately evaluate the effects on crop yield, more work is required taking into consideration different crop types (e.g., maize, wheat, soy) and key processes, e.g., effects of extreme cold on winter wheat growth (Lu et al., 2017), effects of heat stress on maize (Peng et al., 2018), rather than a generic C3-Crop PFT to represent all crops. However, we also note that the simplicity of the representation of crops in ACCESS-ESM1.5 is common across most ESMs (McDermid et al., 2017).

Our study has some additional caveats that need to be acknowledged. The crop albedo enhancement in the southern hemisphere was highest in parts of South America and southeast Australia (Fig. 1), and although reductions in HWF and HWC were statistically significant in these regions (Fig. 5(a) and (d)), the magnitude of the change was relatively small as compared to changes in the northern hemisphere. Although this is consistent with other studies using ESMs (Hirsch et al., 2017; Seneviratne et al., 2018), this result should be treated with caution. Recent studies using regional climate models have shown that ESMs can underestimate the influence of crop albedo enhancement on maximum temperatures by a factor of up to 3 as compared to regional models over Australia, as regional models better resolve agricultural land-use, especially over southwest Western Australia (Kala and Hirsch, 2020). It is likely that effects of crop albedo enhancement on heatwaves for key agricultural regions of the southern hemisphere, such as Australia are higher, however, this needs to be tested using higher resolution ESMs or regional climate models.

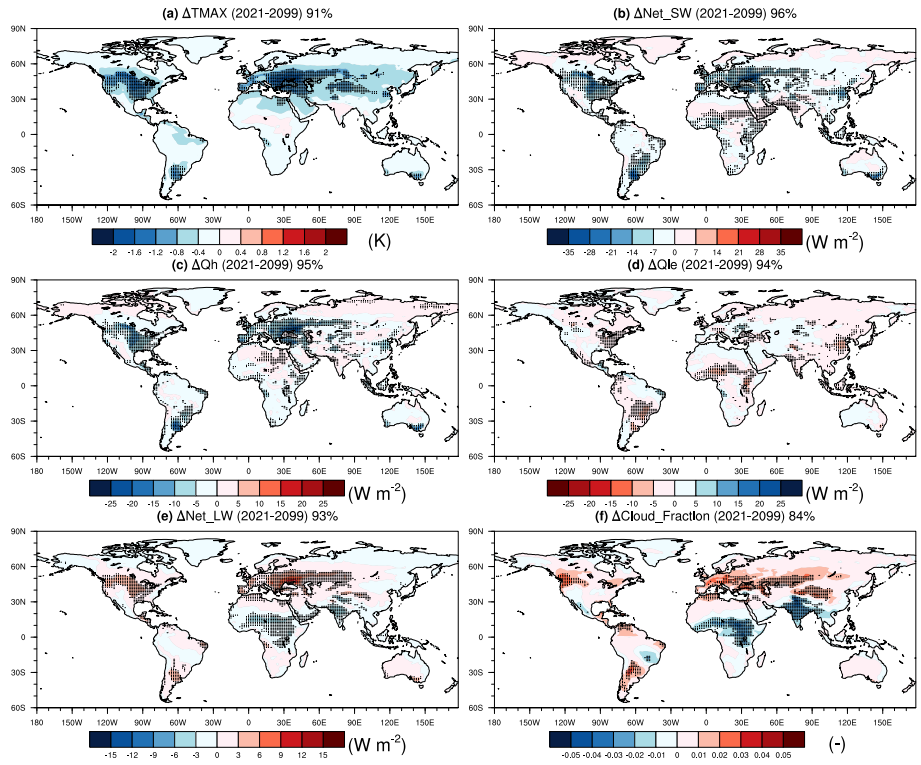

Fig. 7. Same as in Fig. 5, except showing the change in (a) maximum temperature (TMAX); (b) net shortwave radiation (Net_SW); (c) sensible heat flux (Qh); (d) latent heat flux (Qle); (e) net longwave radiation (Net_LW); and, (d) Cloud fraction. The percentages in the titles denote the percentage of grid cells which show a statistically significant difference where the surface albedo was increased (Fig. 1). For example, 90% means that 90% of grid cells which show a statistically significant difference are grid cells where the surface albedo was increased, and hence, 10% of grid cells show a change where there was no increase in crop albedo.

Due to computational and data constraints, we only examined one future climate scenario, SSP2-4.5, which is the "middle of the road" scenario. Additional simulations with SSP5 "fossil-fuelled development" would be helpful to further investigate at what point global warming would essentially dwarf any regional cooling via crop albedo enhancement. This would be especially interesting for the heatwave magnitude, for regions such as North America, where our results show little difference between the simulations towards 2099. Finally, we examined the maximum possible benefits by applying a change in albedo of up to approximately 0.1, which is the upper limit of change in albedo possible with current crop varieties. We also assume that changes happen everywhere, instantly. This is not realistic and crop albedo enhancement would be very difficult to implement in this manner in the real world. However, our results highlight a significant factor that is often not considered in the choice of what crops to grow, and that is the albedo of the crop. The main outcome of this study for policy-makers is that not only should we focus on factors such as drought and heat tolerance of crops, but given two varieties of crops with similar yield performance and tolerance to heat and drought, the crop with lower albedo should be preferred, especially if the crop is to be grown over large areas.

CRediT authorship contribution statement

Jatin Kala: Writing – review & editing, Formal analysis, Conceptualisation, Methodology. **Annette L. Hirsch:** Writing – review & editing, Conceptualisation, Methodology. **Tilo Ziehn:** Writing – review & editing, Conceptualisation, Methodology, Simulations. **Sarah E. Perkins-Kirkpatrick:** Reviewing, Conceptualisation, Methodology. **Martin G. De Kauwe:** Reviewing, Conceptualisation, Methodology. **Andy Pitman:** Reviewing, Conceptualisation, Methodology.

Declaration of competing interest

The authors declare that they have no known competing financial interests or personal relationships that could have appeared to influence the work reported in this paper.

Acknowledgements

The heatwave metrics were computed using Python code provided by Dr. Tammas Loughran at https://github.com/tammasloughran/ehf heatwaves. Jatin Kala is supported by an Australian Research Council Discovery Early Career Researcher Award (DE170100102). Annette L. Hirsch, Andy J. Pitman, Sarah E. Perkins-Kirkpatrick are supported by the Australian Research Council Centre of Excellence for Climate Extremes (CE170100023). Martin G. De Kauwe and Andy J. Pitman acknowledge support from the Australian Research Council Discovery Grant (DP190101823). Sarah E. Perkins-Kirkpatrick is supported by an Australian Research Council Future Fellowship (FT170100106). This research/ project was undertaken with the assistance of resources and services from the National Computational Infrastructure (NCI), which is supported by the Australian Government. We thank Dr Rachel Law and Dr. Ying-Ping Wang from CSIRO for discussions and comments on the manuscript.

References

Allen, M., Dube, O.P., Solecki, W., Aragón-Durand, F., Cramer, W., Humphreys, S., Kainuma, M., Kala, J., Mahowald, N., Mulugetta, Y., Perez, R., Wairiu, M., Zickfeld, K., 2018. Framing and context. In: Masson-Delmotte, V., Zhai, P., Pörtner, H.O., Roberts, D., Skea, J., Shukla, P., Pirani, A., Moufouma-Okia, W., Péan, C., Pidcock, R., Connors, S., Matthews, J.B.R., Chen, Y., Zhou, X., Gomis, M.I., Lonnoy, E., Maycock, T., Tignor, M., Waterfield, T. (Eds.), Global Warming of 1.5 °C. An IPCC Special Report on the Impacts of Global Warming of 1.5 °C Above Pre-Industrial Levels and Related Global Greenhouse Gas Emission Pathways, in the Context of Strengthening the Global Response to the Threat of Climate

Change, Sustainable Development, and Efforts to Eradicate Poverty. URL: https://www.ipcc.ch/sr15/chapter/chapter-1/.

Asseng, S., Ewert, F., Martre, P., Rötter, R.P., Lobell, D.B., Cammarano, D., Kimball, B.A., Ottman, M.J., Wall, G.W., White, J.W., Reynolds, M.P., Alderman, P.D., Prasad, P.V.V., Aggarwal, P.K., Anothai, J., Basso, B., Biernath, C., Challinor, A.J., De Sanctis, G., Doltra, J., Fereres, E., Garcia-Vila, M., Gayler, S., Hoogenboom, G., Hunt, L.A., Izaurralde, R.C., Jabloun, M., Jones, C.D., Kersebaum, K.C., Koehler, A.K., Müller, C., Naresh Kumar, S., Nendel, C., O'Leary, G., Olesen, J.E., Palosuo, T., Priesack, E., Eyshi Rezaei, E., Ruane, A.C., Semenov, M.A., Shcherbak, I., Stöckle, C., Stratonovitch, P., Streck, T., Supit, I., Tao, F., Thorburn, P.J., Waha, K., Wang, E., Wallach, D., Wolf, J., Zhao, Z., Zhu, Y., 2015. Rising temperatures reduce global wheat production. Nature Clim. Change 5 (2), 143–147. http://dx.doi.org/10.1038/nclimate2470.

Bi, D., Dix, M., Marsland, S.J., O'Farrell, S., Rashid, H.A., Uotila, P., Hirst, A.C., Kowalczyk, E., Golebiewski, M., Sullivan, A., Yan, H., Hannah, N., Franklin, C., Sun, Z., Vohralik, P., Watterson, I., Zhou, X., Fiedler, R., Collier, M., Ma, Y., Noonan, J., Stevens, L., Uhe, P., Zhu, H., Griffies, S.M., Hill, R., Harris, C., Puri, K., 2013. The ACCESS coupled model: description, control climate and evaluation. Aust. Meteorol. Oceanogr. J. 63, 41–64.

Breuer, L., Eckhardt, K., Frede, H.-G., 2003. Plant parameter values for models in temperate climates. Ecol. Model. 169 (2), 237–293. http://dx.doi.org/10.1016/S0304-3800(03)00274-6, URL: https://www.sciencedirect.com/science/article/pii/S0304380003002746.

Brovkin, V., Petoukhov, V., Claussen, M., Bauer, E., Archer, D., Jaeger, C., 2009. Geoengineering climate by stratospheric sulfur injections: Earth system vulnerability to technological failure. Clim. Change 92 (3), 243–259. http://dx.doi.org/10.1007/s10584-008-9490-1.

Chambers, J., 2020. Global and cross-country analysis of exposure of vulnerable populations to heatwaves from 1980 to 2018. Clim. Change 163 (1), 539–558. http://dx.doi.org/10.1007/s10584-020-02884-2.

Davin, E.L., Seneviratne, S.I., Ciais, P., Olioso, A., Wang, T., 2014. Preferential cooling of hot extremes from cropland albedo management. Proc. Natl. Acad. Sci. 111 (27), 9757. http://dx.doi.org/10.1073/pnas.1317323111, URL: http://www.pnas.org/content/111/27/9757.abstract.

Dee, D.P., Uppala, S.M., Simmons, A.J., Berrisford, P., Poli, P., Kobayashi, S., Andrae, U., Balmaseda, M.A., Balsamo, G., Bauer, P., Bechtold, P., Beljaars, A.C.M., van de Berg, L., Bidlot, J., Bormann, N., Delsol, C., Dragani, R., Fuentes, M., Geer, A.J., Haimberger, L., Healy, S.B., Hersbach, H., Hólm, E.V., Isaksen, L., Kållberg, P., Köhler, M., Matricardi, M., McNally, A.P., Monge-Sanz, B.M., Morcrette, J.J., Park, B.K., Peubey, C., de Rosnay, P., Tavolato, C., Thépaut, J.N., Vitart, F., 2011. The ERA-Interim reanalysis: configuration and performance of the data assimilation system. Q. J. R. Meteorol. Soc. 137 (656), 553–597. http://dx.doi.org/10.1002/qj.828.

Febrero, A., Fernández, S., Molina-Cano, J.L., Araus, J.L., 1998. Yield, carbon isotope discrimination, canopy reflectance and cuticular conductance of barley isolines of differing glaucousness. J. Exp. Botany 49 (326), 1575–1581. http://dx.doi.org/10.1093/jxb/49.326.1575.

Fischer, E.M., Schär, C., 2010. Consistent geographical patterns of changes in high-impact European heatwaves. Nat. Geosci. 3 (6), 398–403. http://dx.doi.org/10.1038/ngeo866.

Genesio, L., Bassi, R., Miglietta, F., 2021. Plants with less chlorophyll: A global change perspective. Global Change Biol. 27 (5), 959–967. http://dx.doi.org/10.1111/gcb.15470, URL: https://onlinelibrary.wiley.com/doi/abs/10.1111/gcb.15470.

Grant, R.H., Heisler, G.M., Gao, W., Jenks, M., 2003. Ultraviolet leaf reflectance of common urban trees and the prediction of reflectance from leaf surface characteristics. Agric. Forest Meteorol. 120 (1), 127–139. http://dx.doi.org/10.1016/j.agrformet.2003.08.025, URL: https://www.sciencedirect.com/science/article/pii/S0168192303001904.

Griffies, S.M., 2014. Elements of the Modular Ocean Model (MOM) (2012 release with update). GFDL Ocean Group Technical report No. 7, NOAA/GFDL, p. 632 + xiii, URL: https://mom-ocean.github.io/assets/pdfs/MOM5_manual.pdf.

Hatfield, J.L., Carlson, R.E., 1979. Light quality distributions and spectral albedo of three maize canopies. Agric. Meteorol. 20 (3), 215–226. http://dx.doi.org/10.1016/0002-1571(79)90022-0, URL: https://www.sciencedirect.com/science/article/pii/0002157179900220.

Herold, N., Ekström, M., Kala, J., Goldie, J., Evans, J.P., 2018. Australian climate extremes in the 21st century according to a regional climate model ensemble: Implications for health and agriculture. Weather Clim. Extrem. 20, 54–68. http://dx.doi.org/10.1016/j.wace.2018.01.001, URL: https://www.sciencedirect.com/science/article/pii/S221209471730169X.

Hirsch, A.L., Prestele, R., Davin, E.L., Seneviratne, S.I., Thiery, W., Verburg, P.H., 2018. Modelled biophysical impacts of conservation agriculture on local climates. Global Change Biol. 24 (10), 4758–4774. http://dx.doi.org/10.1111/gcb.14362.

Hirsch, A.L., Ridder, N.N., Perkins-Kirkpatrick, S.E., Ukkola, A., 2021. CMIP6 Multi-Model evaluation of present-day heatwave attributes. Geophys. Res. Lett. 48 (22), e2021GL095161. http://dx.doi.org/10.1029/2021GL095161, URL: https://agupubs.onlinelibrary.wiley.com/doi/abs/10.1029/2021GL095161.

Hirsch, A.L., Wilhelm, M., Davin, E.L., Thiery, W., Seneviratne, S.I., 2017. Can climate-effective land management reduce regional warming? J. Geophys. Res. Atmos. 122 (4), 2269–2288. http://dx.doi.org/10.1002/2016jd026125.

Hunke, E.C., Lipscomb, W.H., 2010. CICE: The Los Alamos sea ice model documentation and software user's manual. Version 4.1. LA-CC-06-012, Los Alamos National Laboratory, NM, URL: https://csdms.colorado.edu/w/images/CICE_documentation_and_software_user%27s_manual.pdf.

Hurtt, G.C., Chini, L., Sahajpal, R., Frolking, S., Bodirsky, B.L., Calvin, K., Doelman, J.C., Fisk, J., Fujimori, S., Klein Goldewijk, K., Hasegawa, T., Havlik, P., Heinimann, A., Humpenöder, F., Jungclaus, J., Kaplan, J.O., Kennedy, J., Krisztin, T., Lawrence, D., Lawrence, P., Ma, L., Mertz, O., Pongratz, J., Popp, A., Poulter, B., Riahi, K., Shevliakova, E., Stehfest, E., Thornton, P., Tubiello, F.N., van Vuuren, D.P., Zhang, X., 2020. Harmonization of global land use change and management for the period 850–2100 (LUH2) for CMIP6. Geosci. Model Dev. 13 (11), 5425–5464. http://dx.doi.org/10.5194/gmd-13-5425-2020, URL: https://gmd.copernicus.org/articles/13/5425/2020/.

Jyoteeshkumar reddy, P., Sharples, J.J., Lewis, S.C., Perkins-Kirkpatrick, S.E., 2021. Modulating influence of drought on the synergy between heatwaves and dead fine fuel moisture content of bushfire fuels in the southeast Australian region. Weather Clim. Extrem. 31, 100300. http://dx.doi.org/10.1016/j.wace.2020.100300, URL: https://www.sciencedirect.com/science/article/pii/S2212094720303133.

Kala, J., De Kauwe, M.G., Pitman, A.J., Medlyn, B.E., Wang, Y.-P., Lorenz, R., Perkins-Kirkpatrick, S.E., 2016. Impact of the representation of stomatal conductance on model projections of heatwave intensity. Sci. Rep. 6 (1), 23418. http://dx.doi.org/10.1038/srep23418.

Kala, J., Evans, J.P., Pitman, A.J., Schaaf, C.B., Decker, M., Carouge, C., Mocko, D., Sun, Q., 2014. Implementation of a soil albedo scheme in the CABLEv1.4b land surface model and evaluation against MODIS estimates over Australia. Geosci. Model Dev. 7 (5), 2121–2140. http://dx.doi.org/10.5194/gmd-7-2121-2014, URL: https://gmd.copernicus.org/articles/7/2121/2014/.

Kala, J., Hirsch, A.L., 2020. Could crop albedo modification reduce regional warming over Australia?. Weather and Climate Extremes 30, 100282. http://dx.doi.org/10.1016/j.wace.2020.100282, https://www.sciencedirect.com/science/article/pii/S2212094719302385.

Keith, D.W., 2000. Geoengineering the climate: History and prospect. Annu. Rev. Energy Environ. 25 (1), 245–284. http://dx.doi.org/10.1146/annurev.energy.25.1.245.

Klimenko, V.V., Ginzburg, A.S., Fedotova, E.V., Tereshin, A.G., 2020. Heat waves: A new danger for the Russian power system. Dokl. Phys. 65 (9), 349–354. http://dx.doi.org/10.1134/S1028335820090050.

Kowalczyk, E.A., Stevens, L., Law, R.M., Dix, M., Wang, Y.P., Harman, I.N., Haynes, K., Srbinovsky, J., Pak, B., Ziehn, T., 2013. The land surface model component of ACCESS: description and impact on the simulated surface climatology. Aust. Meteorol. Oceanogr. J. 63, 65–82.

Kravitz, B., MacMartin, D.G., Visioni, D., Boucher, O., Cole, J.N.S., Haywood, J., Jones, A., Lurton, T., Nabat, P., Niemeier, U., Robock, A., Séférian, R., Tilmes, S., 2021. Comparing different generations of idealized solar geoengineering simulations in the geoengineering model intercomparison project (geomip). Atmos. Chem. Phys. 21 (6), 4231–4247. http://dx.doi.org/10.5194/acp-21-4231-2021, URL: https://acp.copernicus.org/articles/21/4231/2021/.

Law, R.M., Ziehn, T., Matear, R.J., Lenton, A., Chamberlain, M.A., Stevens, L.E., Wang, Y.P., Srbinovsky, J., Bi, D., Yan, H., Vohralik, P.F., 2017. The carbon cycle in the Australian community climate and earth system simulator (ACCESS-ESM1) – Part 1: Model description and pre-industrial simulation. Geosci. Model Dev. 10 (7), 2567–2590. http://dx.doi.org/10.5194/gmd-10-2567-2017, URL: https://gmd.copernicus.org/articles/10/2567/2017/.

Lawrence, M.G., Schäfer, S., Muri, H., Scott, V., Oschlies, A., Vaughan, N.E., Boucher, O., Schmidt, H., Haywood, J., Scheffran, J., 2018. Evaluating climate geoengineering proposals in the context of the Paris agreement temperature goals. Nature Commun. 9 (1), 3734. http://dx.doi.org/10.1038/s41467-018-05938-3.

Lorenz, R., Pitman, A.J., Donat, M.G., Hirsch, A.L., Kala, J., Kowalczyk, E.A., Law, R.M., Srbinovsky, J., 2014. Representation of climate extreme indices in the ACCESS1.3b coupled atmosphere–land surface model. Geosci. Model Dev. 7 (2), 545–567. http://dx.doi.org/10.5194/gmd-7-545-2014, URL: https://gmd.copernicus.org/articles/7/545/2014/.

Lorenz, R., Pitman, A.J., Sisson, S.A., 2016. Does Amazonian deforestation cause global effects; can we be sure? J. Geophys. Res. Atmos. 121 (10), 5567–5584. http://dx.doi.org/10.1002/2015JD024357.

Lu, Y., Williams, I.N., Bagley, J.E., Torn, M.S., Kueppers, L.M., 2017. Representing winter wheat in the community land model (version 4.5). Geosci. Model Dev. 10 (5), 1873–1888. http://dx.doi.org/10.5194/gmd-10-1873-2017, URL: https://gmd.copernicus.org/articles/10/1873/2017/.

Martin, G.M., Bellouin, N., Collins, W.J., Culverwell, I.D., Halloran, P.R., Hardiman, S.C., Hinton, T.J., Jones, C.D., McDonald, R.E., McLaren, A.J., O'Connor, F.M., Roberts, M.J., Rodriguez, J.M., Woodward, S., Best, M.J., Brooks, M.E., Brown, A.R., Butchart, N., Dearden, C., Derbyshire, S.H., Dharssi, I., Doutriaux-Boucher, M., Edwards, J.M., Falloon, P.D., Gedney, N., Gray, L.J., Hewitt, H.T., Hobson, M., Huddleston, M.R., Hughes, J., Ineson, S., Ingram, W.J., James, P.M., Johns, T.C., Johnson, C.E., Jones, A., Jones, C.P., Joshi, M.M., Keen, A.B., Liddicoat, S., Lock, A.P., Maidens, A.V., Manners, J.C., Milton, S.F., Rae, J.G.L., Ridley, J.K., Sellar, A., Senior, C.A., Totterdell, I.J., Verhoef, A., Vidale, P.L., Wiltshire, A., 2011. The HadGEM2 family of met office unified model climate configurations. Geosci. Model Dev. 4 (3), 723–757. http://dx.doi.org/10.5194/gmd-4-723-2011, URL: https://gmd.copernicus.org/articles/4/723/2011/.

Martin, G.M., Milton, S.F., Senior, C.A., Brooks, M.E., Ineson, S., Reichler, T., Kim, J., 2010. Analysis and reduction of systematic errors through a seamless approach to modeling weather and climate. J. Clim. 23 (22), 5933–5957. http://dx.doi.org/10.1175/2010JCLI3541.1, URL: https://journals.ametsoc.org/view/journals/clim/23/22/2010jcli3541.1.xml.

McDermid, S.S., Mearns, L.O., Ruane, A.C., 2017. Representing agriculture in earth system models: Approaches and priorities for development. J. Adv. Model. Earth Syst. 9 (5), 2230–2265. http://dx.doi.org/10.1002/2016MS000749, URL: https://agupubs.onlinelibrary.wiley.com/doi/abs/10.1002/2016MS000749.

McEvoy, D., Ahmed, I., Mullett, J., 2012. The impact of the 2009 heat wave on melbourne's critical infrastructure. Local Environ. 17 (8), 783–796. http://dx.doi.org/10.1080/13549839.2012.678320.

McMichael, A.J., Lindgren, E., 2011. Climate change: present and future risks to health, and necessary responses. J. Intern. Med. 270 (5), 401–413. http://dx.doi.org/10.1111/j.1365-2796.2011.02415.x, URL: <GotoISI>://WOS:000297021600001.

Meinshausen, M., Nicholls, Z.R.J., Lewis, J., Gidden, M.J., Vogel, E., Freund, M., Beyerle, U., Gessner, C., Nauels, A., Bauer, N., Canadell, J.G., Daniel, J.S., John, A., Krummel, P.B., Luderer, G., Meinshausen, N., Montzka, S.A., Rayner, P.J., Reimann, S., Smith, S.J., van den Berg, M., Velders, G.J.M., Vollmer, M.K., Wang, R.H.J., 2020. The shared socio-economic pathway (SSP) greenhouse gas concentrations and their extensions to 2500. Geosci. Model Dev. 13 (8), 3571–3605. http://dx.doi.org/10.5194/gmd-13-3571-2020, URL: https://gmd.copernicus.org/articles/13/3571/2020/.

Nairn, J.R., Fawcett, R.J.B., 2015. The excess heat factor: A metric for heatwave intensity and its use in classifying heatwave severity. Int. J. Environ. Res. Public Health 12 (1), 227–253. http://dx.doi.org/10.3390/ijerph120100227, URL: https://www.mdpi.com/1660-4601/12/1/227.

Oke, P.R., Griffin, D.A., Schiller, A., Matear, R.J., Fiedler, R., Mansbridge, J., Lenton, A., Cahill, M., Chamberlain, M.A., Ridgway, K., 2013. Evaluation of a near-global eddy-resolving ocean model. Geosci. Model Dev. 6 (3), 591–615. http://dx.doi.org/10.5194/gmd-6-591-2013, URL: https://gmd.copernicus.org/articles/6/591/2013/.

O'Neill, B.C., Tebaldi, C., van Vuuren, D.P., Eyring, V., Friedlingstein, P., Hurtt, G., Knutti, R., Kriegler, E., Lamarque, J.F., Lowe, J., Meehl, G.A., Moss, R., Riahi, K., Sanderson, B.M., 2016. The scenario model intercomparison project (ScenarioMIP) for CMIP6. Geosci. Model Dev. 9 (9), 3461–3482. http://dx.doi.org/10.5194/gmd-9-3461-2016, URL: https://gmd.copernicus.org/articles/9/3461/2016/.

Peng, B., Guan, K., Chen, M., Lawrence, D.M., Pokhrel, Y., Suyker, A., Arkebauer, T., Lu, Y., 2018. Improving maize growth processes in the community land model: Implementation and evaluation. Agric. Forest Meteorol. 250–251, 64–89. http://dx.doi.org/10.1016/j.agrformet.2017.11.012, URL: https://www.sciencedirect.com/science/article/pii/S0168192317303854.

Perkins, S.E., Alexander, L.V., 2013. On the measurement of heat waves. J. Clim. 26 (13), 4500–4517. http://dx.doi.org/10.1175/JCLI-D-12-00383.1, URL: https://journals.ametsoc.org/view/journals/clim/26/13/jcli-d-12-00383.1.xml.

Perkins-Kirkpatrick, S.E., Lewis, S.C., 2020. Increasing trends in regional heatwaves. Nature Commun. 11 (1), 3357. http://dx.doi.org/10.1038/s41467-020-16970-7.

Rohde, R., Muller, R., Jacobsen, R., Perlmutter, S., Rosenfeld, A., Wurtele, J., Curry, J., Wickham, C., Mosher, S., 2013. Berkeley earth temperature averaging process. Geoinform. Geostat. Overv. 1, http://dx.doi.org/10.4172/gigs.1000103.

Rübbelke, D., Vögele, S., 2011. Impacts of climate change on European critical infrastructures: The case of the power sector. Environ. Sci. Policy 14 (1), 53–63. http://dx.doi.org/10.1016/j.envsci.2010.10.007, URL: https://www.sciencedirect.com/science/article/pii/S1462901110001371.

Russo, S., Sillmann, J., Fischer, E.M., 2015. Top ten European heatwaves since 1950 and their occurrence in the coming decades. Environ. Res. Lett. 10 (12), 124003. http://dx.doi.org/10.1088/1748-9326/10/12/124003.

Ruthrof, K.X., Breshears, D.D., Fontaine, J.B., Froend, R.H., Matusick, G., Kala, J., Miller, B.P., Mitchell, P.J., Wilson, S.K., van Keulen, M., Enright, N.J., Law, D.J., Wernberg, T., Hardy, G.E.S.J., 2018. Subcontinental heat wave triggers terrestrial and marine, multi-taxa responses. Sci. Rep. 8 (1), 13094. http://dx.doi.org/10.1038/s41598-018-31236-5.

Seneviratne, S.I., Donat, M.G., Pitman, A.J., Knutti, R., Wilby, R.L., 2016. Allowable CO2 emissions based on regional and impact-related climate targets. Nature 529 (7587), 477–483. http://dx.doi.org/10.1038/nature16542.

Seneviratne, S.I., Phipps, S.J., Pitman, A.J., Hirsch, A.L., Davin, E.L., Donat, M.G., Hirschi, M., Lenton, A., Wilhelm, M., Kravitz, B., 2018. Land radiative management as contributor to regional-scale climate adaptation and mitigation. Nat. Geosci. 11 (2), 88–96. http://dx.doi.org/10.1038/s41561-017-0057-5.

Seneviratne, S.I., Zhang, X., Adnan, M., Badi, W., Dereczynski, C., Di Luca, A., Ghosh, S., Iskandar, I., Kossin, J., Lewis, S., Otto, F., Pinto, I., Satoh, M., Vicente-Serrano, S.M., Wehner, M., Zhou, B., 2021. Weather and climate extreme events in a changing climate. In: Masson-Delmotte, V., Zhai, P., Pirani, A., Connors, S.L., Péan, C., Berger, S., Caud, N., Chen, Y., Goldfarb, L., Gomis, M.I., Huang, M., Leitzell, K., Lonnoy, E., Matthews, J.B.R., Maycock, T.K., Waterfield, T., Yelekçi, O., Yu, R., Zhou, B. (Eds.), Climate Change 2021: The Physical Science Basis. Contribution of Working Group I to the Sixth Assessment Report of the Intergovernmental Panel on Climate Change. Cambridge University Press, URL: https://www.ipcc.ch/report/ar6/wg1/downloads/report/IPCC_AR6_WGI_Chapter_11.pdf.

Sun, W., Wang, B., Chen, D., Gao, C., Lu, G., Liu, J., 2020. Global monsoon response to tropical and arctic stratospheric aerosol injection. Clim. Dynam. 55 (7), 2107–2121. http://dx.doi.org/10.1007/s00382-020-05371-7.

Thiery, W., Davin, E.L., Lawrence, D.M., Hirsch, A.L., Hauser, M., Seneviratne, S.I., 2017. Present-day irrigation mitigates heat extremes. J. Geophys. Res. Atmos. 122 (3), 1403–1422. http://dx.doi.org/10.1002/2016jd025740.

Thiery, W., Visser, A.J., Fischer, E.M., Hauser, M., Hirsch, A.L., Lawrence, D.M., Lejeune, Q., Davin, E.L., Seneviratne, S.I., 2020. Warming of hot extremes alleviated by expanding irrigation. Nature Communications 11 (1), 290. http://dx.doi.org/10.1038/s41467-019-14075-4, https://doi.org/10.1038/s41467-019-14075-4.

Tjiputra, J.F., Grini, A., Lee, H., 2016. Impact of idealized future stratospheric aerosol injection on the large-scale ocean and land carbon cycles. J. Geophys. Res. Biogeosci. 121 (1), 2–27. http://dx.doi.org/10.1002/2015JG003045.

Uddin, M.N., Marshall, D.R., 1988. Variation in epicuticular wax content in wheat. Euphytica 38 (1), 3–9. http://dx.doi.org/10.1007/BF00024805.

Valcke, S., 2013. The OASIS3 coupler: a European climate modelling community software. Geosci. Model Dev. 6 (2), 373–388. http://dx.doi.org/10.5194/gmd-6-373-2013, URL: https://gmd.copernicus.org/articles/6/373/2013/.

van der Velde, M., Wriedt, G., Bouraoui, F., 2010. Estimating irrigation use and effects on maize yield during the 2003 heatwave in France. Agric. Ecosyst. Environ. 135 (1), 90–97. http://dx.doi.org/10.1016/j.agee.2009.08.017, URL: https://www.sciencedirect.com/science/article/pii/S0167880909002618.

Wang, Y.P., Kowalczyk, E., Leuning, R., Abramowitz, G., Raupach, M.R., Pak, B., van Gorsel, E., Luhar, A., 2011. Diagnosing errors in a land surface model (CABLE) in the time and frequency domains. J. Geophys. Res. Biogeosci. 116 (G1), http://dx.doi.org/10.1029/2010JG001385.

Wang, Y.P., Law, R.M., Pak, B., 2010. A global model of carbon, nitrogen and phosphorus cycles for the terrestrial biosphere. Biogeosciences 7 (7), 2261–2282. http://dx.doi.org/10.5194/bg-7-2261-2010, URL: https://bg.copernicus.org/articles/7/2261/2010/.

Wang, Y.P., Leuning, R., 1998. A two-leaf model for canopy conductance, photosynthesis and partitioning of available energy I:: Model description and comparison with a multi-layered model. Agric. Forest Meteorol. 91 (1), 89–111. http://dx.doi.org/10.1016/S0168-1923(98)00061-6, URL: https://www.sciencedirect.com/science/article/pii/S0168192398000616.

Westerling, A.L., Hidalgo, H.G., Cayan, D.R., Swetnam, T.W., 2006. Warming and earlier spring increase western U.S. forest wildfire activity. Science 313 (5789), 940–943. http://dx.doi.org/10.1126/science.1128834.

Wilhelm, M., Davin, E.L., Seneviratne, S.I., 2015. Climate engineering of vegetated land for hot extremes mitigation: An earth system model sensitivity study. J. Geophys. Res. Atmos. 120 (7), 2612–2623. http://dx.doi.org/10.1002/2014JD022293.

Wilks, D.S., 2006. On "field significance" and the false discovery rate. J. Appl. Meteorol. Climatol. 45 (9), 1181–1189. http://dx.doi.org/10.1175/JAM2404.1, URL: https://journals.ametsoc.org/view/journals/apme/45/9/jam2404.1.xml.

Ziehn, T., Chamberlain, M.A., Law, R.M., Lenton, A., Bodman, R.W., Dix, M., Stevens, L., Wang, Y.-P., Srbinovsky, J., 2020. The Australian earth system model: ACCESS-ESM1.5. J. South. Hemisph. Earth Syst. Sci. 70 (1), 193–214, URL: https://doi.org/10.1071/ES19035.

Ziehn, T., Lenton, A., Law, R.M., Matear, R.J., Chamberlain, M.A., 2017. The carbon cycle in the Australian community climate and earth system simulator (ACCESS-ESM1) – Part 2: Historical simulations. Geosci. Model Dev. 10 (7), 2591–2614. http://dx.doi.org/10.5194/gmd-10-2591-2017, URL: https://gmd.copernicus.org/articles/10/2591/2017/.

Update

Weather and Climate Extremes

Volume , Issue , , Page

DOI: https://doi.org/10.1016/j.wace.2022.100428

Weather and Climate Extremes xxx (xxxx) xxx

Contents lists available at ScienceDirect

Weather and Climate Extremes

journal homepage: www.elsevier.com/locate/wace

Corrigendum to "Assessing the potential for crop albedo enhancement in reducing heatwave frequency, duration, and intensity under future climate change" [Weather Clim. Extrem. 35 (2022) 100415]

Jatin Kala [a,b,*], Annette L. Hirsch [b], Tilo Ziehn [c], Sarah E. Perkins-Kirkpatrick [e,b], Martin G. De Kauwe [d,b], Andy Pitman [b]

[a] Environmental and Conservation Sciences, Centre for Climate-Impacted Terrestrial Ecosystems, Harry Butler Institute, Murdoch, University, Murdoch, WA, 6150, Australia
[b] Australian Research Council Centre of Excellence for Climate Extremes, University of New South Wales, NSW, 2052, Australia
[c] Commonwealth Scientific and Industrial Research Organisation, Aspendale, VIC, 3195, Australia
[d] School of Biological Sciences, University of Bristol, Bristol, BS8 1TQ, UK
[e] School of Science, University of New South Wales, Canberra, ACT, Australia

The authors regret to inform readers of a typographical error in the last sentence of the conclusion. The word "lower" should instead have been "higher" as follows:

The main outcome of this study for policymakers is that not only should we focus on factors such as drought and heat tolerance of crops, but given two varieties of crops with similar yield performance and tolerance to heat and drought, the crop with **higher** albedo should be preferred, especially if the crop is to be grown over large areas.

The authors would like to apologise for any inconvenience caused.

DOI of original article: https://doi.org/10.1016/j.wace.2022.100415.

* Corresponding author. Environmental and Conservation Sciences, Centre for Climate-Impacted Terrestrial Ecosystems, Harry Butler Institute, Murdoch, University, Murdoch, WA, 6150, Australia.

E-mail address: J.Kala@murdoch.edu.au (J. Kala).

https://doi.org/10.1016/j.wace.2022.100428

Available online 28 February 2022